Talanta 85 (2011) 130–135

Contents lists available at ScienceDirect

Talanta

journal homepage: www.elsevier.com/locate/talanta

Highly conducting gold nanoparticles–graphene nanohybrid films for ultrasensitive detection of carcinoembryonic antigen

Jing Han, Ying Zhuo*, Ya-Qin Chai, Li Mao, Ya-Li Yuan, Ruo Yuan*

Education Ministry Key Laboratory on Luminescence and Real-Time Analysis, College of Chemistry and Chemical Engineering, Southwest University, Chongqing 400715, PR China

ARTICLE INFO

Article history:
Received 5 December 2010
Received in revised form 9 March 2011
Accepted 17 March 2011
Available online 31 March 2011

Keywords:
Gold nanoparticles–graphene (Au–Gra)
Chitosan-ferrocene and nano-TiO_2 (CS-Fc + TiO_2)
Amperometric immunosensor
Carcinoembryonic antigen (CEA)

ABSTRACT

A new label-free amperometric immunosensor was developed for detection of carcinoembryonic antigen (CEA) based on chitosan-ferrocene (CS-Fc) and nano-TiO_2 (CS-Fc + TiO_2) complex film and gold nanoparticles–graphene (Au–Gra) nanohybrid. CS-Fc + TiO_2 composite membrane was first modified on a bare glass carbon electrode. Then Au–Gra nanohybrid was formed on the CS-Fc + TiO_2 membrane by self-assembly strategy. Next, further immobilization of anti-CEA was constructed according to the strong interaction between Au–Gra and the amido groups of anti-CEA. Since Au–Gra nanohybrid films provided a congenial microenvironment for the immobilization of biomolecules, the surface coverage of antibody protein could be enhanced and the sensitivity of the immunosensor has been improved. The good electronic conductive characteristic might be attributed to the synergistic effect of graphene nanosheets and Au NPs. The modified process was characterized by scanning electron microscope (SEM) and cyclic voltammetry (CV). Under optimized conditions, the resulting biosensor displayed good amperometric response to CEA with linear range from 0.01 to 80 ng/mL and a detection limit of 3.4 pg/mL (signal/noise = 3). The results demonstrated that the immunosensor has advantages of high conduction, sensitivity, and long life time. This assay approach showed a great potential in clinical applications and detection of low level proteins.

© 2011 Elsevier B.V. All rights reserved.

1. Introduction

A variety of approaches and strategies for the protein immobilization have been developed based on the extensive application of nanomaterials in biosensor fabrication [1]. As well known, gold nanoparticles (Au NPs) have many unique properties such as high surface free energy, strong adsorption ability, well suitability and good conductivity [2,3]. Besides, it can provide more binding sites and more congenial microenvironment for biomolecules immobilization to retain the bioactivity of the proteins, which can prolong the life time of biosensor [4,5]. Furthermore, graphene has been investigated extensively in recent years because of its two-dimensional (2D) sheet of carbon atoms in a hexagonal construction with atoms bonded by sp2 bonds [6], which results in the extraordinary properties [7,8] of large surface area, good mechanical properties, highly electrical conductivity [9–11]. As a result, graphene was considered as a "rising star" in the field of materials science and condensed matter physics.

In recent years, many studies of carbon-based metal nanocomposites have been reported, as the interesting electrical, optical, and magnetic properties [12,13] are usually superior to those of the carbon or metal species [14]. In our previous work [15], a functionalized gold/carbon nanotube composite nanohybrid was developed by electrochemical reduction of Au^{3+} for the immobilization of antibody. Recently Zhang and co-workers successfully prepared glucose biosensor based on Au NPs functionalized graphene by electrodeposition method [16]. However, it is rarely reported work regarding the synthesis of gold nanoparticles–graphene nanohybrid (Au–Gra) and the application of it as protein matrix for immunosensor construction [17,18]. Therefore, the Au–Gra was directly synthesized in this work by one step, which is according the green method of reduction of graphene oxid (GO) and gold chloride ($HAuCl_4$) by L-ascorbic acid (L-AA) in water at room temperature [19]. On the other hand, due to its simple preparation, low cost, short response time, accurate and sensitive platform, label-free electrochemical immunosensor has become one of the most powerful methods for protein detection [20,21]. At the same time, to avoid the pollution of the analyte solution, the immobilization of redox pairs on the electrode surface has been major strategy to construct a label-free amperometric immunosensors. It is well known that chitosan (CS) is an attractive natural cationic biopolymer obtained from partial deacetylation of chitin. It possesses excellent film-forming ability, biocompatibility, good adhesion, non-toxicity, and susceptibility to chemical modification due to the presence of plentiful amino groups [22] and ferrocenemonocar-

* Corresponding authors at: Tel.: +86 23 68252277, fax: +86 23 68252277.
E-mail addresses: yingzhuo@swu.edu.cn (Y. Zhuo), yuanruo@swu.edu.cn (R. Yuan).

0039-9140/$ – see front matter © 2011 Elsevier B.V. All rights reserved.
doi:10.1016/j.talanta.2011.03.036

boxylic (Fc-COOH) is an ideal electrochemical probe with efficient electrochemical redox-activity [23,24]. Thus, with the help of EDC and NHS, Fc-COOH group was covalently bounded to CS to obtain a novel redox active chitosan-branched ferrocene (CS-Fc) complex. In order to further enhance the stability of composite membrane and increase the surface area, TiO_2 was introduced in CS-Fc solution. Then the TiO_2 doped chitosan-branched ferrocene complex film (CS-Fc + TiO_2) was constructed with desirable properties.

Carcinoembryonic antigen (CEA) is a kind of glycoprotein with a molecular weight of about 200 kDa in colorectal carcinomas. And it is an important tumor marker for clinical diagnosis of colorectal, gastric, pancreatic, and cervical carcinomas and others [25]. Furthermore, the CEA level in serum is also related to the state of tumor. Therefore, the detection of CEA is very essential. Compared with conventional immunoassay methods for CEA quantitative determination, such as enzyme-linked immunosorbent assay (ELISA) [26], radioimmunoassay (RIA) [27], and chemiluminescence immunoassay (CLIA) [28], the electrochemical immunosensor has been one of attractive analytical methods due to potential utility such as specific, simple, direct detection techniques and reductions in cost and real-time of analysis compared with conventional immunoassay techniques. Herein, we successfully constructed a CEA amperometric immunosensor based on the combining of CS-Fc + TiO_2 complex film and Au–Gra nanostructural composite. With the good biocompatibility and excellent redox-activity, the CS-Fc + TiO_2 composite solution was first coated on the surface of bare GCE. Then Au–Gra nanostructural composite was further adsorbed on the resulting electrode through the well-developed interaction between Au NPs and amino groups of CS. At last, anti-CEA was immobilized on the desirable interface of Au–Gra nanostructural composite. Experiment results showed that the amperometric response of the immunosensor decreased with the increase of the CEA concentration. Details of the preparation, characterization and possible application of immunosensor are described in the experimental section below.

2. Experimental

2.1. Reagents

Graphene oxide sheets were obtained in Pioneer Nanotechnology Co. (Nanjing, China). Bovine serum albumin (BSA, 96–99%). N-hydroxy succinimide (NHS) and N-(3-dimethylaminopropyl)-N′-ethylcarbodiimidehydrochloride (EDC) were purchased from Shanghai Medpep Co. Ltd. (Shanghai, China). Carcinoembryonic antigen (CEA, human carcinoembyonic antigen) and carcinoembryonic antibody (anti-CEA, monoclonal antibody) were provided by Biocell Company (Zhengzhou, China). Ferrocenemonocarboxylic (Fc-COOH), Chitosan (CS, 99% deacetylation), Titania nanoparticles (nano-TiO_2, 5%), gold chloride ($HAuCl_4$) and L-ascorbic acid (L-AA) were obtained from Sigma Chemical Co. (St. Louis, MO, USA). All other materials used were of the highest quality available and purchased from regular sources. Double distilled water was used throughout this study. $LiClO_4$–glycine buffer, pH 6.86 (0.05 M) was used throughout this experiment.

2.2. Apparatus

Cyclic voltammetric (CV) measurements were carried out with a CHI 660C Electrochemical Workstation (Shanghai ChenHua Instrument, China). A three-electrode electrochemical cell was composed of a modified glass carbon electrode (GCE, Ø = 4 mm) as the working electrode, a platinum wire as the auxiliary electrode, and a saturated calomel electrode (SCE) as the reference electrode. The scanning electron micrographs were taken with a scanning electron microscope (SEM, S-4800, Hitachi, Tokyo, Japan). The size of gold nanoparticles was estimated from transmission electron microscopy (TEM) (H600, Hitachi Instrument, Japan). The pH measurements were made with a digital ion analyzer (Model PHS-3C, Dazhong Instruments, Shanghai, China).

2.3. Preparation of Fc-CS + TiO_2

The synthesis of the nanocomposite was performed in the following method. In the first step, 0.5 g ferrocene was dissolved in 2.5 mL double distilled water under continual stirring. And then 0.5 mL EDC and NHS (4:1) mixture solution was added to the ferrocene solution and stirred for overnight aiming at activation the carboxyl of Fc-COOH. Next, 100 mL chitosan solution (1%) was obtained by fully dissolving 1.0 g chitosan in 100 mL acetic acid solution with sonication approach. Subsequently, 300 μL chitosan solution (1%) was mixed with 1 mL the prepared Fc-COOH solution under continuous stirring for 4 h. Finally, 300 μL nano-TiO_2 (5%) was added to the mixed solution and then stirred for 0.5 h to obtain the homogenous CS-Fc + TiO_2 solution.

2.4. Preparation of Au-Gra nanohybrid

Graphene oxide sheets were first dissolved by ultrasonication in water. Then 5 mg L-AA was added to 5 mL (0.1 mg/mL) of an aqueous dispersion of the GO and stirred for 12 h at ambient condition. Subsequently, 2 mL chloroauric acid ($HAuCl_4$, 1%) was added to this mixture, and it was stirred for overnight. At last, in order to remove excessive graphite oxide and L-AA, the synthesis of gold nanoparticles–graphene nanohybrid was centrifugally washed extensively with bi-distilled water and finally dispersed in 5 mL of double distilled water.

2.5. Fabrication of modified electrodes

To obtain mirror like surface, the glass carbon electrode (GCE, Ø = 4 mm) was carefully polished with 0.3 and 0.05 μm alumina powder separately prior to fabrication of the immunosensor. Then the electrode was chemically cleaned by immersing into freshly prepared 2:1 mixture of H_2SO_4 and H_2O_2 for 30 s. After a short rinse with distilled water and ultrasonic cleaning with distilled water and ethanol, the GCE was allowed to dry at room temperature.

To construct the anti-CEA/Au–Gra/CS-Fc + TiO_2 immunosensor, 10 μL prepared CS-Fc + TiO_2 composite solution was first dropped on the pretreated GCE electrode and dried in air for 2 h. Then 10 μL Au–Gra composite was coated on CS-Fc + TiO_2 composite modified electrode. Following that, the obtained electrode was incubated in 0.5 mL anti-CEA solution at 4 °C for 12 h. In order to block possible remaining active sites and avoid the non-specific adsorption, 20 μL of 0.25% BSA solution was dropped on the electrode for 20 min at 35 °C. After every step, the modified electrode was thoroughly cleaned with doubly distilled water. The finished immunosensor was stored at 4 °C when not in use. The schematic diagram of the stepwise self-assemble procedure of the immunosensor was shown in Fig. 1.

3. Results and discussion

3.1. Characterization of the modified electrode surface

The surface topographies of the nanocomposite formed films were investigated using scanning electronic microscope (SEM) with images shown in Fig. 2. A homogeneous morphology was observed at CS-Fc + TiO_2 nanocomposite membrane modified surface as shown in Fig. 2(A). After Au–Gra was assembled onto the surface of the CS-Fc + TiO_2 film, the modified surface reveals many Au NPs

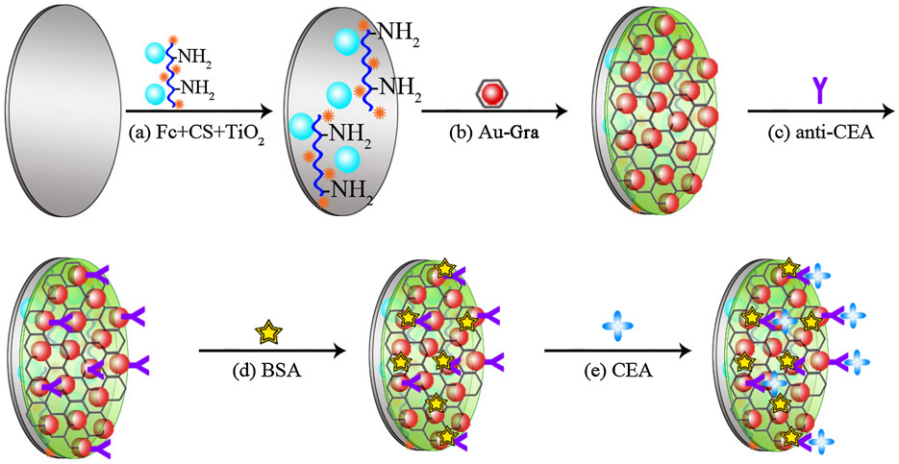

Fig. 1. Schematic illustration of the stepwise immunosensor fabrication process: (a) fabrication of CS-Fc + TiO_2 monolayer; (b) formation of Au–Gra monolayer; (c) anti-CEA loading; (d) blocking with 0.25% BSA; (e) incubation with CEA.

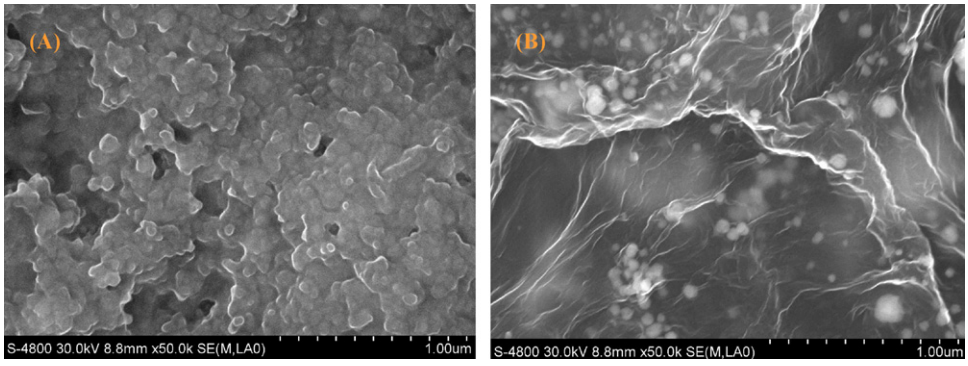

Fig. 2. (A) SEM image of the CS-Fc + TiO_2 composite film; (B) SEM image of Au–Gra/CS-Fc + TiO_2.

wrapped with a layer of thin film of graphene with the typical crumpled and wrinkled structure coating on the surface of hybrid membrane. The Au NPs integrate uniformly with the graphene forming the Au–Gra nanohybrid films as shown in Fig. 2(B).

3.2. CV characterization of modified electrodes

Cyclic voltammograms (CVs) of different modified electrodes were performed in 0.05 mol/L $LiClO_4$–glycine buffer (pH 6.86) from −0.2 to 0.6 V (vs. SCE) at a scan rate of 50 mV/s as shown in Fig. 3. No obvious redox peaks were observed at bare GCE in the potential range in $LiClO_4$–glycine solution (curve a) as the lack of redox mediator. After CS-Fc + TiO_2 was coated on the GCE surface and the resulting electrode showed a stable and well-defined redox peaks at 0.24 and 0.38 V vs. SCE (curve b), indicating ferrocene has good electrochemical activity. With the dropping of Au–Gra solution, the redox peak currents increase significantly, which was ascribed to the good conductivity of gold nanoparticles–graphene (curve c). When the electrode was modified with anti-CEA, the peak current was decreased (curve d). Subsequently, the immunosensor was blocked with 0.25% BSA solution and then incubated in an incubation solution containing 60 ng/mL CEA. It could be found that the peak currents of the curves (e) and (f) were decreased comparing with curve (d). The reason for this was that the insulating BSA and CEA protein layers on the electrode retards the electron transfer. On the basis of CV results, we might make a conclusion that the anti-CEA could be successfully immobilized on the base electrode.

Fig. 4 shows the CVs of the prepared immunosensor in 0.05 mol/L $LiClO_4$–glycine solution (pH 6.86) from −0.2 to 0.6 V (vs. SCE) at different scan rates. It can be found that both the anodic and cathodic peak currents were increased as the scan rates in the range from 20 to 700 mV/s. In addition, the peak current versus the square of root of sweep rate plot, shown in the inset, exhibits a linear relationship, suggesting that the reaction is a diffusion-controlled process.

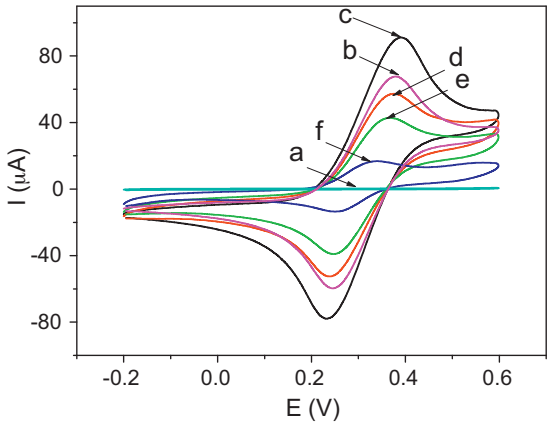

Fig. 3. Cyclic voltammograms performed in 0.05 mol/L $LiClO_4$–glycine (pH 6.86). (a) Bare GCE; (b) CS-Fc + TiO_2 modified GCE electrode; (c) Au–Gra/CS-Fc + TiO_2 modified GCE electrode; (d) anti-CEA/Au–Gra/CS-Fc + TiO_2 modified GCE electrode; (e) anti-CEA/Au–Gra/CS-Fc + TiO_2 modified GCE electrode blocked with 0.25% BSA; (f) modified GCE electrode after incubation with 60 ng/mL CEA. The scan rate was 50 mV/s.

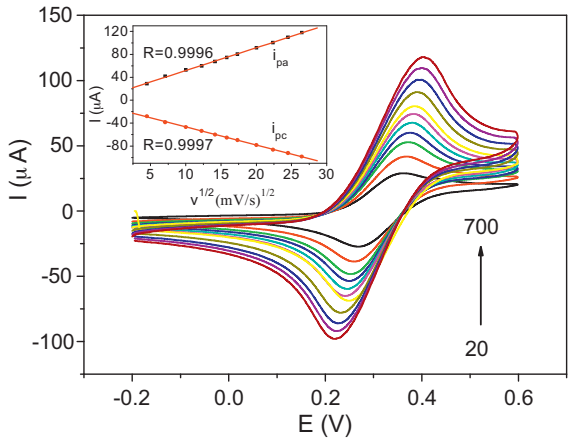

Fig. 4. Cyclic voltammograms of the modified electrode at different scan rates (from inner to outer): 20, 50, 100, 150, 200, 250, 300, 400, 500, and 600 and 700 mV/s in 0.05 mol/L $LiClO_4$–glycine. (pH 6.86) All potentials are given versus SCE. The inset shows the dependence of the redox peak currents on the square root of scan rates.

3.3. Optimization of analytical conditions

3.3.1. Influences of pH of the $LiClO_4$–glycine buffer

It was well known that the pH of the solution has a profound effect on the amperometric responses. In order to optimize the pH, a series of $LiClO_4$–glycine solutions with the pH from 4.0 to 9.0 were prepared and the immunosensors were tested by CVs. It was found that the amperometric responses increased in the pH range from 4.0 to 6.5 and then decreased as pH increase further (Fig. 5(A)). The experimental results indicated that the maximum response occurs at pH 6.5. At the same time, it can be found the responses at pH 6.5 and pH 7.0 having no significant difference. Thus, we chose pH of 6.86 as the optimal pH in the further study.

3.3.2. Effect of temperature on the immunoreactions

As well known, incubation temperature is an important factor for the reaction between the antigen and the antibody. Fig. 5(B) shows the effect of temperature on the performance of the immunosensor from 15 to 50 °C. The current responses showed a rapidly decrease to 35 °C and after that it increased with the temperature over 35 °C. That means it would take 35 °C to form the most immunocomplexes between the analyte antigens in the incubating solution and antibodies on the electrode surface. Therefore, incubation temperature of 35 °C was adopted as the optimum immunoreaction temperature.

3.3.3. Effect of incubation time on the immunoreactions

The effect of the immunochemical incubation time on response signals was also studied. Fig. 5(C) reveals the influence of incubation time of the immunoassay. The modified electrode was immersed in 20 ng/mL CEA for 1, 3, 5, 8, 10, 12, 15 and 20 min, respectively. The current response obtained decreased with the incubation time rapidly up to 10 min and then tended to level off. Thus, 10 min was adopted as the optimal incubation time for subsequent study.

3.4. Performance of the immunosensor

3.4.1. CV response and calibration curve

The proposed immunosensor was incubated with varying amounts of CEA, and then it was carried to the test cell with 0.05 mol/L $LiClO_4$–glycine buffer solution. And the typical CV plots were recorded in Fig. 6(A). It can be observed the response signal decreased with the increasing CEA concentrations. The calibration plot for the CEA detection of the resulting immunosensor under

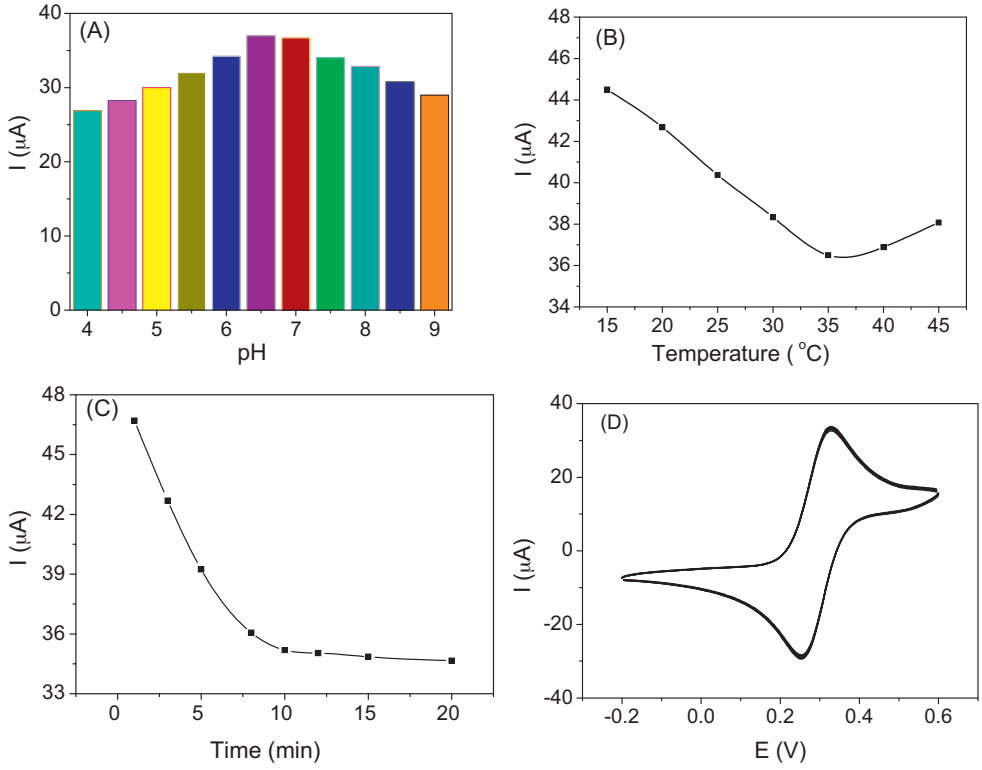

Fig. 5. (A) pH dependency of the anodic peak currents responses for the inmunosensor in 0.05 mol/L $LiClO_4$–glycine (pH 6.86) at 50 mV/s scan rate. All potentials are given versus SCE. (B) Influence of the incubation temperature on amperometric response of immunosensor when immune-reacted with 20 ng/mL CEA. (C) The effect of the different incubation time after the immunosensor incubated with 20 ng/mL CEA solution in 0.05 mol/L $LiClO_4$–glycine (pH 6.86) at 50 mV/s. (D) Stability of the obtained immunosensor incubated with 20 ng/mL CEA examined after 100 CV circles.

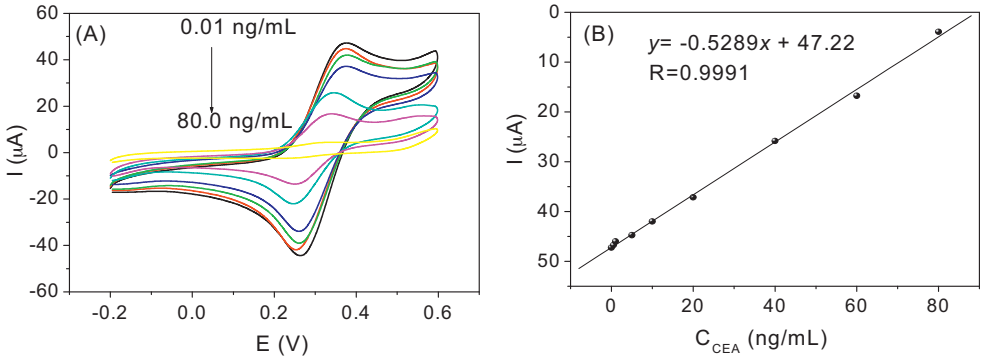

Fig. 6. Curve (A) reveals: The typical cyclic voltammograms plots upon the addition of varying amounts of CEA. All potentials are given versus SCE and the scan rate was 50 mV/s Curve (B) shows: The calibration plots of the anodic peak current response versus concentration of CEA with the immunosensor under optimal conditions.

Table 1
Possible interferences tested with the proposed immunosensor.

Experiment		Amperometric responses (μA)[a]	Ratio of current (I_c/I_b)
Standard CEA solution[b]	CEA	36.64	–
Interfering solution[c]	CEA (CA 125)	37.18	1.0147
	CEA (CA 19-9)	37.39	1.0205
	CEA (CA 15-3)	35.97	0.9817
	CEA (AFP)	36.92	1.0076
	CEA (BSA)	36.01	0.9828
	CEA (Ascorbic acid)	36.98	1.0093
	CEA (L-cysteine)	36.24	0.9891
	CEA (L-glutamate)	36.35	0.9921
	CEA (L-lysine)	36.98	1.0093
	CEA (Dopamine)	37.25	1.0167

[a] Each amperometric measurement under the same conditions.
[b] The standard CEA solution consists of 20 ng/mL CEA.
[c] The interfering solution consists of 20 ng/mL CEA and 20 ng/mL different interfering agents.

optimal experimental conditions was illustrated in Fig. 6(B). A linear dependence of the amperometric response with CEA concentration was found over the 0.01–80.0 ng/mL ($R = 0.9991$), with the equation of $y = -0.5289x + 47.22$ and a detection limit of 3.4 pg/mL at a signal/noise ratio of 3. The results indicated that the method is a useful method for quantifying CEA, which showed the potential applications value in clinical.

3.4.2. Reproducibility and stability

The reproducibility of the response of the immunosensors was examined by analysis of the same concentration of CEA (20 ng/mL) using five equally prepared electrodes. The five immunosensors, made independently, showed the current responses of 37.76, 38.62, 37.89, 39.24, 36.77 μA. It was observed that the immunosensor had acceptable reproducibility with a relative standard deviation of 2.45% (less than 5.0%.).

The stability of the immunosensor was also investigated. According to our experimental results and the literature reports [29], $LiClO_4$–glycine solution is a relative acceptable buffer solution with higher current response and better stability, which compared with PBS, HAc-NaAc and KCl–glycine solutions. Thus, we selected $LiClO_4$–glycine to evaluate the stability of the immunosensor. The experiment result was shown in Fig. 5(D). After 100 circles of CV scans in $LiClO_4$–glycine buffer solution, an anodic peak current RSD of 3.27% was acquired. The good stability may contribute to the Au–Gra composite membrane on the electrode surface that could adsorb protein molecules firmly.

3.4.3. Selectivity

In order to evaluate selectivity of the developed immunosensor for CEA, the changes in the current responses induced by some possible interference, such as CA 125, CA 19-9, CA 15-3, AFP, BSA, ascorbic acid, L-cysteine, L-glutamate, L-lysine, dopamine was measured (the test solution containing 20 ng/mL CEA and 20 ng/mL interfering substance) The test results showed that above tested interference would not cause observable interference to determination of CEA, which was attributed to the good selectivity of antigen–antibody immunoreactions. Based on this result, it was confirmed that the fabricated immunosensor constitutes an appropriate tool for the detection of CEA (Table 1).

3.4.4. Analysis of human serum samples

To further evaluate the possibility of the developed electrochemical immunosensors for testing real samples, human serum samples were assessed using the electrochemical immunoassay and a commercially available enzyme-linked immunosorbent assay (ELISA) as a reference method. Six clinical serum specimens supplied by the Ninth People's Hospital of Chongqing, China, were

Table 2
Experimental results comparison of two methods obtained in serum samples.

Serum samples	1	2	3	4	5	6
ELISA (ng/mL)[a]	0.66	5.12	13.21	38.85	65.70	90.24
Immunosensor (ng/mL)[a]	0.71	4.80	13.97	41.17	60.24	85.96
Relative deviation (%)	7.58	−6.25	5.75	5.97	−8.31	−4.74

[a] The values shown here are the average values from three measurements.

determined here. The results are listed in Table 2. The relative deviation of these results is between −8.31% and 7.58%. This finding revealed a good agreement between the both analytical methods.

4. Conclusions

In this study, a new label-free amperometric immunosensor for detection of CEA was successfully developed by immobilization anti-CEA on the Au–Gra/CS-Fc + TiO_2 nanocomposite multi-membrane. The experimental results found that the Au–Gra composite membrane was compact, stable, biocompatible, and liable to promote electron transfer as compared with gold nanoparticles or graphene solely. Moreover, this immunosensor had a good sensitivity and stability, long life time, low detection limit and wide linear range to CEA detection. In general, this paper provide a simple and sensitive method for protein diagnostics in clinical as well as for bioanalysis.

Acknowledgements

The authors are grateful for the financial support by the NNSF of China (21075100), the Ministry of Education of China (Project 708073),Chongqing Key Laboratory on Luminescence and Real-Time Analysis (CSTC, 2006CA8006), the Natural Science Foundation Project of Chongqing (CSTC, 2010BB4121), the Fundamental Research Funds for the Central Universities (XDJK2010C062, XDJK2009B013), the Doctor Foundation of Southwest University (SWU109016) and the Outstanding Youth Foundation of College of Chemistry and Chemical Engineering, Southwest University, China (SWUC009).

References

[1] A. de la Escosura-Muniz, A. Parolo, C. Merkoci, Mater. Today 13 (2010), 7–8 and 17–27.
[2] E. Boisselier, D. Astruc, Chem. Soc. Rev. 38 (2009) 1759–1782.
[3] J. Perez-Juste, I. Pastoriza-Santos, L.M. Liz-Marzan, P. Mulvaney, Coord. Chem. Rev. 249 (2005) 1870–1901.
[4] S.G. Penn, L. He, M.J. Natan, Curr. Opin. Chem. Biol. 7 (2003) 609–615.
[5] G.H. Lu, L.E. Ocola, J.H. Chen, Appl. Phys. Lett. 94 (2009) 083111.
[6] Martin Pumera, Adriano Ambrosi, Alessandra Bonanni, Elaine Lay Khim Chng, Hwee Ling Poh, TrAC 29 (2010) 954–965.
[7] C.N.R. Rao, A.K. Sood, K.S. Subrahmanyam, A. Govindaraj, Angew. Chem. Int. Ed. 48 (2009) 7752.
[8] G. Eda, M. Chhowalla, Nano Lett. 9 (2009) 814–818.
[9] J.T. Robinson, F.K. Perkins, E.S. Snow, Z.Q. Wei, P.E. Sheehan, Nano Lett. 8 (2008) 3137–3140.
[10] A.K. Geim, Science 324 (2009) 1530–1534.
[11] L.D. Kaner, Science 320 (2008) 1170–1171.
[12] O.C. Compton, S.T. Nguyen, Small 6 (2010) 711–723.
[13] X.M. Zhao, B.H. Zhang, K.L. Ai, G. Zhang, L.Y. Cao, X.J. Liu, H.M. Sun, H.S. Wang, L.H. Liu, J. Mater. Chem. 19 (2009) 5547–5553.
[14] Y.F. Ma, S.R. Ali, A.S. Dodoo, H.X. He, J. Phys. Chem. B 110 (2006) 16359–16365.
[15] Y. Zhuo, R. Yuan, Y.Q. Chai, C.L. Hong, Analyst 135 (2010) 2036–2042.
[16] Y.J. Hu, J. Jin, P. Wu, H. Zhang, C.X. Cai, Electrochim. Acta 56 (2010) 491–500.
[17] Y. Fang, S. Guo, C. Zhu, Y. Zhai, E. Wang, Langmuir 26 (2010) 11277.
[18] W. Hong, H. Bai, Y. Xu, Z. Yao, Z. Gu, G. Shi, J. Phys. Chem. C 114 (2010) 1822.
[19] J.L. Zhang, H.J. Yang, G.X. Shen, P. Cheng, J.Y. Zang, S.W. Guo, Chem. Commun. 46 (2010) 1112–1114.
[20] L.P. Qiu, C.C. Wang, P. Hu, Z.S. Wu, G.Li. Shen, R.Q. Yu, Talanta 83 (2010) 42–47.
[21] B. Piro, Q.D. Zhang, S. Reisberg, V. Noel, L.A. Dang, H.T. Duc, M.C. Pham, Talanta 82 (2010) 608–612.
[22] J.H. Lin, W. Qu, S.S. Zhang, Anal. Biochem. 36 (2007) 288.
[23] M. Okochi, H. Ohta, T. Tanaka, T. Matsunaga, Biotechnol. Bioeng. 90 (2005) 14–19.
[24] V.B. Kandimalla, V.S. Tripathi, H.X. Ju, Biomaterials 27 (2006) 1167–1174.
[25] G. Borras, R. Molina, J. Xercavins, A. Ballesta, J. Iglesias, Gynecol. Oncol. 57 (1995) 205–211.
[26] M.Y. Liu, C.P. Jia, Q.H. Jin, X.H. Lou, S.H. Yao, J.Q. Xiang, J.L. Zhao, Talanta 81 (2010) 1625–1629.
[27] D.M.P. Thomson, J. Krupey, S.O. Freedman, P. Gold, Proc. Natl. Acad. Sci. 64 (1969) 161–167.
[28] J.H. Lin, F. Yan, H.X. Ju, Clin. Chim. Acta 341 (2004) 109–115.
[29] Y. Zhuo, P.X. Yuan, R. Yuan, Y.Q. Chai, C.L. Hong, Biomaterials 29 (2008) 1501–1508.